Structural properties and the effect of interaction of alkali (Li +, Na +, K +) and alkaline earth (Be 2+, Mg 2+, Ca 2+) metal cations with G and SG−tetrads

ARTICLE *in* COMPUTATIONAL AND THEORETICAL CHEMISTRY · NOVEMBER 2011

Impact Factor: 1.55 · DOI: 10.1016/j.comptc.2011.07.012

3 AUTHORS, INCLUDING:

Palanisamy Deepa
Manonmaniam Sundaranar University
21 PUBLICATIONS **65** CITATIONS
SEE PROFILE

K. Senthilkumar
Bharathiar University
78 PUBLICATIONS **1,445** CITATIONS
SEE PROFILE

Computational and Theoretical Chemistry 974 (2011) 57–65

Contents lists available at SciVerse ScienceDirect

Computational and Theoretical Chemistry

journal homepage: www.elsevier.com/locate/comptc

Structural properties and the effect of interaction of alkali (Li^+, Na^+, K^+) and alkaline earth (Be^{2+}, Mg^{2+}, Ca^{2+}) metal cations with G and SG-tetrads

P. Deepa, P. Kolandaivel *, K. Senthilkumar

Department of Physics, Bharathiar University, Coimbatore 641 046, India

ARTICLE INFO

Article history:
Received 27 June 2011
Accepted 11 July 2011
Available online 29 July 2011

Keywords:
Alkali
Alkaline earth metals
Interaction energy
Metal ion affinity
Electrostatic potential map

ABSTRACT

The interaction between alkali (Li^+, Na^+, K^+) and alkaline earth (Be^{2+}, Mg^{2+}, Ca^{2+}) metal cations with G and SG-tetrads were studied using ab initio and density functional theory methods. The calculations reveal that cation-G and SG-tetrad complexes adopt normal four-stranded Hoogsteen bonded structures. The substitution of different cations on G and SG-tetrads, affect the geometries and charge distributions. The gas phase binding sequence between the cations-G and SG-tetrads follows the interaction energy and metal ion affinity stability order Li^+>Na^+>K^+, Be^{2+}>Mg^{2+}>Ca^{2+}. The smaller ions are tightly bonded to G and SG-tetrads suggest the domination of electrostatic interaction in the cation–tetraplexes systems. The solvent interaction with the molecular systems has increased the stability of the G, SG-tetrads and their complexes. The two and three-body interaction energies have been used to analyze the influence of a metal cation on the stability of tetrads. Electrostatic potential map of the tetrads have been plotted and the binding of cations have also been shown. Atoms in Molecules theory (AIM) have been performed to study the hydrogen bonds in the metal interacting complexes.

1. Introduction

Guanine (G) tetrads represent an unusual, yet important assembly of nucleic acid bases, which was investigated by fiber X-ray crystallography about 40 years ago, even though they had discovered much earlier [1]. Now they are an active area of research again, since they are important building blocks of DNA and RNA tetraplex structures [2–4]. Tetraplex, which forms sequences of motifs occur in telomeres at the ends of linear chromosomes. The function of telomeres is maintenance of the structural integrity of the genome and insurance of complete replication at the chromosome termini. Similar sequence motifs do also occur in regulatory regions of oncogenes. Tetrads also play an interesting role in supra-molecular chemistry, for example, guanosine analogs perform self-assembly in columnar aggregates in the presence of cations [5]. Zahler and co-workers [6] demonstrated in 1991 that K^+ cation stabilized G-quadruplex structure, able to inhibit telomerase, G-quadruplex DNA has emerged as an attractive target for telomerase inhibitors. Perhaps the most interesting characteristic of these structures is their selective interaction with certain cations that fit well in the cavities formed by stacking of guanine tetrads [7].

The 6-thioguanine (SG) is a known anticancer agent which is readily incorporated in the place of guanine during DNA replication. The incorporation of SG nucleotides into DNA and RNA by polymerase can lead to cell death. The replacement of oxygen by sulfur atom at the O6 position of guanine blocks the formation of hydrogen bond, which is necessary for normal G-tetrad formation and could lead to changes in telomere stability [7]. Stefi et al. [8] have performed large scale molecular dynamics simulations to investigate the ability of the four-stranded guanine DNA motif to incorporate nonstandard guanine analog bases, and they found that the incorporation of 6-thioguanine and 6-thiopurine destabilized four stranded G-DNA structure. The metal binding properties of thio and oxo guanines are different [9] and it has been found that the existence of interactions with a metal ion is essential for the formation of the G-tetrad complexes [10–16]. The presence of ammonium ion stabilizing the G-tetraplex has also been studied [17]. Monovalent cations stabilize the tetraplexes in the order K^+>Na^+>Li^+ [1,12,17]. On the basis of experimental observations, the preferential binding of K^+ versus Na^+ or Li^+ in guanine tetraplexes has been observed and it is an optimal fit of the cation between the two guanine tetrads [18]. The melting point of tetrad forming guanosine gels increases significantly in the presence of alkali metal ions [1] and molecular dynamics trajectories of tetraplex structures revealed that the structures are unstable if cations are absent [19]. The mechanism of cation dependent conformational change of G-rich oligonucleotides has been studied for drug delivery [20].

Ab initio study of the G-tetrad in the absence of cations has shown that, the G-tetrad is stabilized by bifurcated hydrogen bonds [21]. To understand how the different types of cations

* Corresponding author. Tel.: +91 (0) 422 2428441; fax: +91 (0) 422 2422387.
E-mail addresses: ponkvel@buc.edu.in, ponkvel@bu.edu.in (P. Kolandaivel).

2210-271X/$ - see front matter © 2011 Elsevier B.V. All rights reserved.
doi:10.1016/j.comptc.2011.07.012

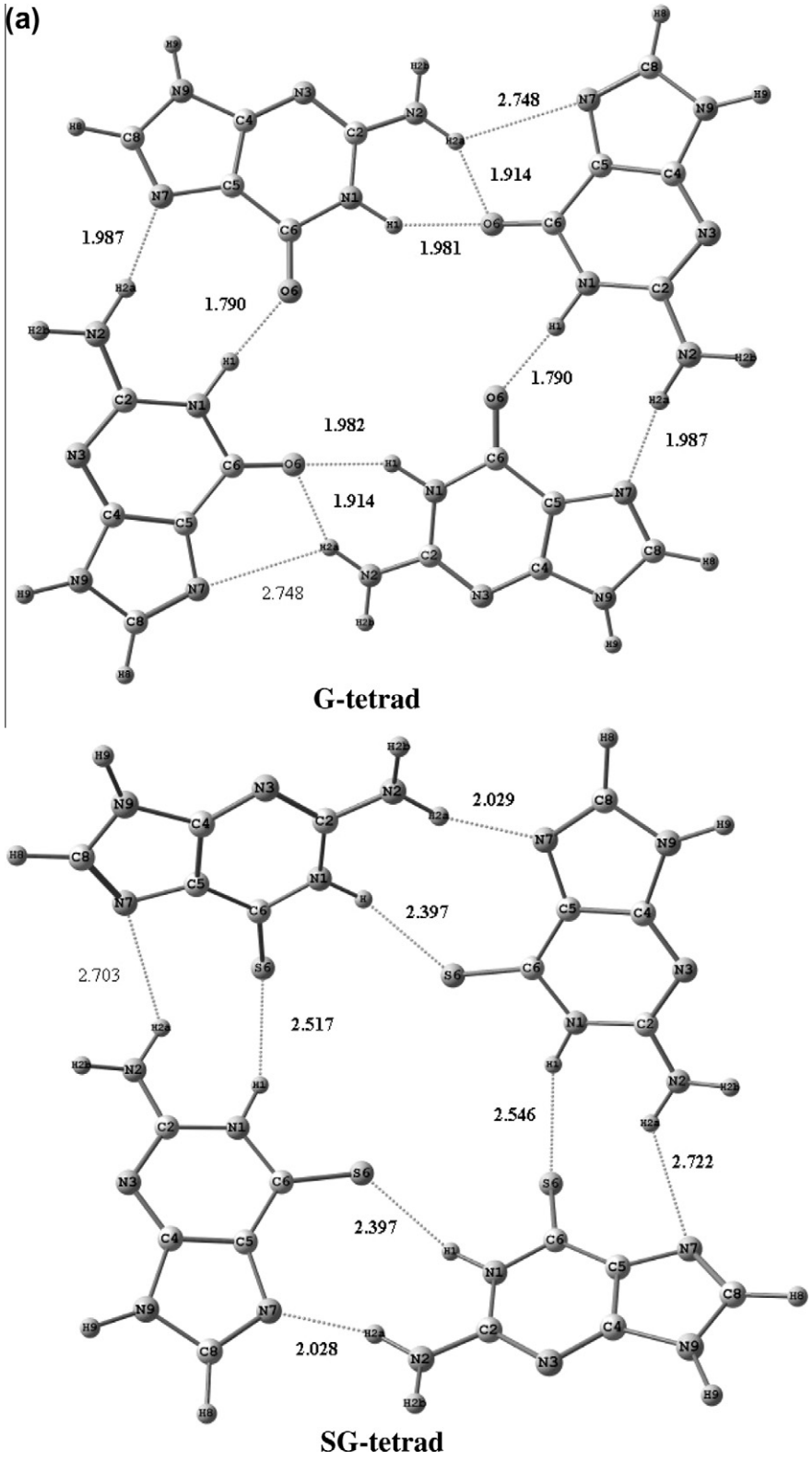

Fig. 1. The structures of G, SG-tetrads and their alkali, alkaline earth metal interacting complexes optimized at B3LYP/6-311G** level of theory. (IUPAC number has been followed for labeling of atoms).

influence the structure of the G-tetraplex, it is necessary to investigate their interactions with the G-tetrad [22]. Previous studies indicate that the crucial role of water in stabilizing the proton transfer in guanine [23,24] and in changing the molecular geometries of GC complexes [25,26]. Many theoretical studies [1,5–7,17–20] have been carried out to study the influence of alkali metal ion with G and SG-tetrads. But still the theoretical study on interaction of G and SG-tetrads with alkaline earth metal ions is lagging. Moreover, the divalent alkaline earth metals are rather more reactive than alkali metals and they react as the alkali metals do, and more. They can coordinate with mono- and bi-dentate ligands. From alkaline earth metals magnesium is the major intracellular

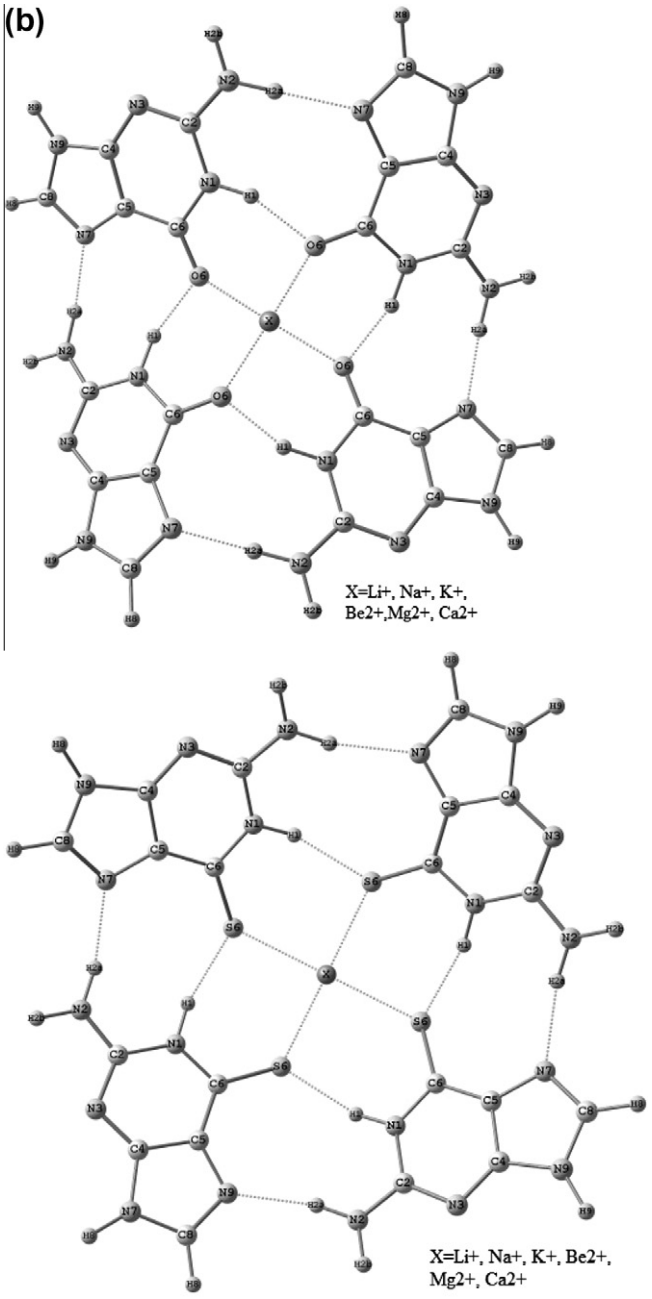

Fig. 1 (*continued*)

divalent ion and is present in all DNA and RNA activation processes. Mg^{2+} cations can act as bridge between specific enzymes and nucleotides, nucleosides and its derivatives [27]. Hence in the present study along with alkali metal, alkaline earth metals have been interacted with G and SG-tetrads.

In continuation to our previous work on the interaction of tautomeric forms of GC base pairs with water molecules [28], the interaction of usual and mismatch base pairs with anticancer drugs like 5-fluorouracil and hydroxyurea [29] the interaction of 2,6-diaminoanthraquinone on G-tetrad, non-G-tetrads and mixed tetrads [30], the interaction of transition metal ions with 8-azaxanthinato salts [31], this work is concerned with the investigation of interactions between the alkali (Li^+, Na^+, K^+) and alkaline earth (Be^{2+}, Mg^{2+}, Ca^{2+}) metal cations with G and SG-tetrads using ab initio and density functional theory methods. The present study is focused on the following aspects: (i) to analyze the influence of metal cations on the structures of the G and SG-tetrads, (ii) to find the stabilizing sequence of the alkali (Li^+, Na^+, K^+) and alkaline earth (Be^{2+}, Mg^{2+}, Ca^{2+}) metal cations in the above tetrads. The influence of solvent on the structural properties of the G and SG-tetrads has been studied. Further, we have examined the interaction energies of inter-molecular hydrogen bonds and its role in providing stability to the complexes. Besides, we have investigated the O–H···O, N–H···O, N–H···S hydrogen bonds and C–O/S···M (M = Li^+, Na^+, K^+, Be^{2+}, Mg^{2+}, Ca^{2+}) interactions present in the complexes using the topological aspects of the electron density distribution based on AIM theory. Electrostatic potential map of the tetrads have been plotted and the binding of cations have also been studied.

2. Computational approach

The earlier studies [22] of hydrogen bonded systems involving DNA bases have shown that the B3LYP method, predicts reliable interaction energies and is compatible with the MP2 method [32]. The Becke's three parameter (B3) exchange functional along with the Lee–Yang–Parr's (LYP) gradient corrected correlation functional [33,34] represented as B3LYP of density functional theory (DFT) method with 6-311G** basis set have been used to optimize G and SG-tetrads and their metal cation interacting complexes. In order to achieve more rigorous energy comparison for the G, SG-tetrad and their complexes, MP2/6-311G** single point energy calculation has been performed for the geometries optimized by B3LYP/6-311G** level of theory. Vibrational frequency calculations show that all the optimized tetrads and metal cation interacting complexes are real minima without imaginary frequencies. Single point energy calculations have been performed to study the solute–solvent interaction using the self-consistent reaction field theory (SCRF) [35] at B3LYP/6-311G** level of theory. This method is based on Tomasi's polarized continuum model (PCM), which defines the cavity as the union of a series of interlocking atomic spheres.

The interaction energies have been corrected for the basis set superposition error (BSSE) using counterpoise correction method [36]. Since the role of individual energy components of interaction energy is important to analyze the metal cations, G and SG-tetrads, the many body analysis [37] have been performed, by partitioning the interaction energy into two and five body interactions,

$$\Delta E_{TOTAL} = E_{(ABCDE)} - [E_{(A)} + E_{(B)} + E_{(C)} + E_{(D)} + E_{(E)}]$$

$$\Delta^5 E(ABCDE) = \Delta E_{TOTAL} - [\Delta^2 E(AB) + \Delta^2 E(AC) + \Delta^2 E(BC) + \Delta^2 E(AD) + \Delta^2 E(AE)\Delta^2 E(BD) + \Delta^2 E(BE) + \Delta^2 E(CD) + \Delta^2 E(CE) + \Delta^2 E(DE)]$$

$$\Delta^2 E(AB) = E_{AB} - [E_{(A)} + E_{(B)}]$$

where $E_{(ABCDE)}$ is the total energy of metal cation interacting complexes and E_A, E_B, E_C, E_D, E_E, are the total energy of single base or metal cations and E_{AB} is the total energy of any two interacting molecules (base pairs or base with metal cations). Atoms in Molecules (AIM) theory [38–41] applied to many systems involving nucleic acid, nucleic base pairing [39], guanine tetrad [40] and metal cations with complexes has proved itself to be a valuable tool. The Metal Ion Affinity (MIA) considered as the negative of the enthalpy for the process has been calculated as

$$MIA = -[E_{el}(BM)^+ - E_{el}(B) - E_{el}(M^+) + (E_{vib}(BM^+) - E_{vib}(B))]$$

where E_{el} is the electronic energy obtained from the SCF computation, and E_{vib} includes the zero point energy and temperature corrections from 0 to 298 K [42–45]. Electron density and Laplacian of electron density has been calculated at B3LYP/6-311G** level of

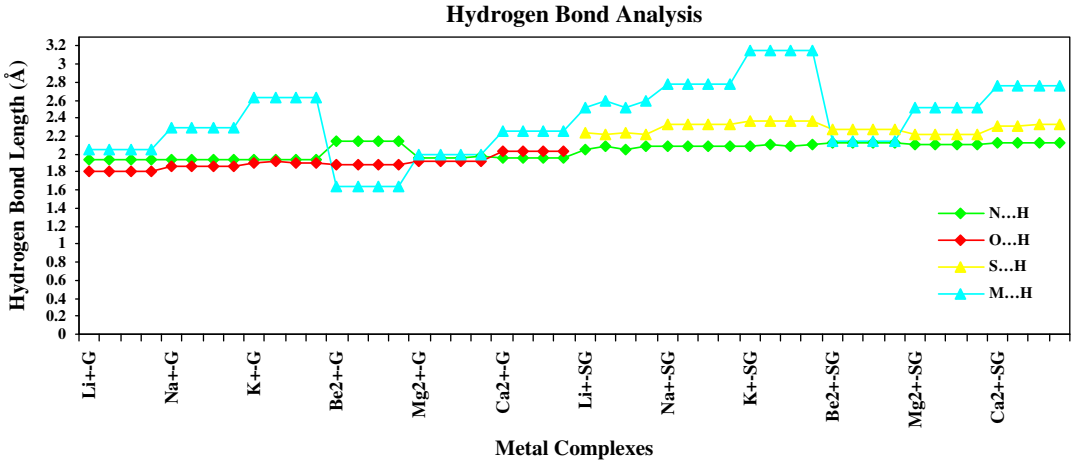

Fig. 2. The metal complexes versus hydrogen bond length (Å).

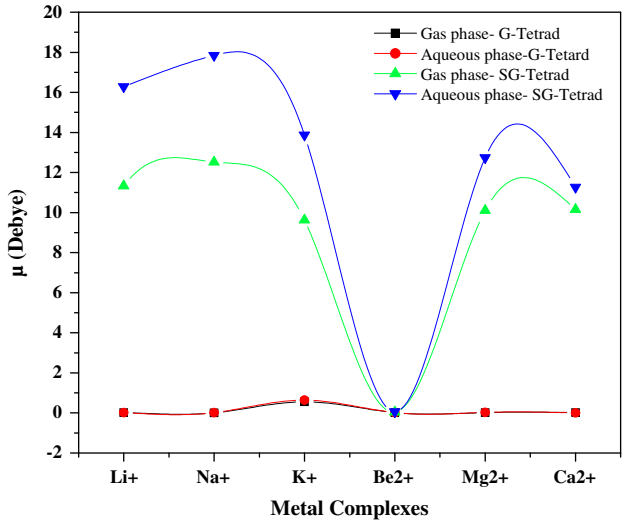

Fig. 3. Dipole moment (in Debye) of G, SG-tetrads and their metal cation interacting complexes in gas and aqueous phases calculated at B3LYP/6-311G** level of theory.

theory. All these calculations have been performed using the Gaussian 03W package [46].

3. Results and discussion

3.1. Geometries

The optimized structures of the G, SG-tetrads and their interaction with alkali and alkaline earth metal ions have been calculated at B3LYP/6-311G** level of theory are depicted in Fig. 1 and S1. The N2–H2, N1–H1 and C=O bond lengths of guanine monomer are 1.008, 1.011, 1.211 Å, the N2–H2, N1–H1 and C=S bond lengths of 6-thioguanine (SG) monomer are 1.008, 1.013, 1.663 Å at B3LYP/6-311G** level of theory respectively. The corresponding bond lengths in G and SG-tetrads get elongated by about 0.02 Å. In G and SG-tetrads the donor group atoms are O6, S6 and N7, and the acceptor group atoms are H1 and H2. The two inter-base hydrogen bond lengths O6···H1 and N7···H2 in G-tetrad are 1.790, 1.982 Å and 1.987, 2.748 Å respectively. The corresponding hydrogen bond lengths S6···H1 and N7···H2 in SG-tetrad are 2.397, 2.546 Å and 1.966, 1.969 Å respectively. As predicted by Meng et al. [7] the differences between the geometries of G and SG-tetrads are due to the larger radius of sulfur atom present in the SG-tetrads, as a result less compact structures are formed.

In addition to the interactions within the tetrad, stacking and backbone interactions with other bases, the presence of metal ions and solvent effects do affect the nucleic acid structure and stability. The calculated hydrogen bond lengths were presented in Fig. S1 as Supplementary Material. The N–H···N type hydrogen bonds in the G and SG-tetrads are relatively strong with bond length in the range of 1.932–2.098 Å for alkali metal ions and 1.952–2.147 Å for alkaline earth metal ions. The N–H···O type hydrogen bonds in the G and SG-tetrads is in the range of 1.807–2.373 Å for alkali metal ions and 1.888–2.322 Å for alkaline earth metal ions. In the present study no bifurcated hydrogen bonds are formed in the G and SG-tetrads with metal cations as observed by Gu and Leszczynski [22]. The presence of a cation in the guanine-tetrad adopts the normal four-stranded Hoogsteen-bonded G-tetrad structure. More pronounced changes in the structures have been observed for the interaction of K^+ and Ca^{2+} complexes in G and SG-tetrads due to the influence of metal ions. In the case of G and SG-tetrads, the N1–H1···N7, N1–H1···O6 and N1–H1···S6 hydrogen bonds get strengthen by the interaction of metal cations, indicating the stability of the complexes. The size of the cations influences the structural parameters of the cation–G and SG-tetrad complexes. Also, the hydrogen bonds are weakened following the increase in the size of the cations from Li^+ to K^+ and from Be^{2+} to Ca^{2+} complexes. While comparing alkali and alkaline earth metal cations as moving from Li^+ to Be^{2+} complexes, the hydrogen bonds are also found to be weakened. The hydrogen bond analysis graph of G and SG-tetrads are shown in Fig 2.

The interactions among the oxygen atoms in the central part of the G-tetrad, which repel each other due to the electrostatic interactions, the tetrad adopts the bifurcate hydrogen bond. The high charge density in the small Li^+ cation results in a stronger electrostatic attraction. The bond length of the O6–C6 in G-tetrad and S6–C6 in SG-tetrad increases as the radius of the metal cation decreases. The above bond lengths are found to elongate 0.02 Å for alkali metals and 0.06 Å for alkaline earth metal complexes. As the metal ions moves from alkali to alkaline earth metal cations the O6–C6 and S6–C6 bond lengths in tetrads are found to be weakened. Ross and Hardin [47] suggested that the K^+ may increase the electron delocalization in the guanine aromatic system and enhance the inner hydrogen bonding. The changes in the N1–H1···O6 and N1–H1···S6 bond lengths in the tetrads suggest that the presence of a cation does enhance the hydrogen bonding.

The total energies and dipole moments of the tetrads and their metal cation interacting complexes in the gas and aqueous phases

Table 1
Interaction energies ΔE (in kcal/mol) of alkali and alkaline earth metals with G-tetrad complexes and their respective isolated G-tetrad.

Base Pair	ΔE Kcal/mol		Base Pair	ΔE Kcal/mol		Base Pair	ΔE Kcal/mol	
	B3lyp	Mp2		B3lyp	Mp2		B3lyp	Mp2
G-Li^+			G-Na^+			G-K^+		
Δ^2E_{iso}	−76.09	−74.91	Δ^2E_{iso}	−76.09	−74.91	Δ^2E_{iso}	−76.09	−74.91
ΔE_{Tot}	−205.48	−209.69	ΔE_{Tot}	−184.21	−188.29	ΔE_{Tot}	−158.00	−153.43
$\Delta^2E^{com}_{(G1^+Li^+)}$	−50.19	−46.36	$\Delta^2E^{com}_{(G1^+Na^+)}$	−37.19	−33.99	$\Delta^2E^{com}_{(G1+K^+)}$	−26.45	−24.71
$\Delta^2E^{com}_{(G2^+Li^+)}$	−50.14	−46.31	$\Delta^2E^{com}_{(G2^+Na^+)}$	−37.19	−33.99	$\Delta^2E^{com}_{(G2^+K^+)}$	−26.76	−24.58
$\Delta^2E^{com}_{(G3^+Li^+)}$	−50.26	−46.41	$\Delta^2E^{com}_{(G3^+Na^+)}$	−37.22	−34.01	$\Delta^2E^{com}_{(G3^+K^+)}$	−26.87	−24.67
$\Delta^2E^{com}_{(G4^+Li^+)}$	−50.14	−46.31	$\Delta^2E^{com}_{(G4^+Na^+)}$	−37.23	−34.02	$\Delta^2E^{com}_{(G4^+K^+)}$	−26.77	−24.58
Δ^2E_{G1G2}	−10.65	−11.46	Δ^2E_{G1G2}	−12.84	−13.36	Δ^2E_{G1G2}	−13.45	−13.87
Δ^2E_{G1G3}	0.05	−0.36	Δ^2E_{G1G3}	−1.09	−1.34	$^2E_{G1G3}$	−1.41	−1.57
Δ^2E_{G1G4}	−10.66	−11.46	Δ^2E_{G1G4}	−12.83	−13.35	Δ^2E_{G1G4}	−13.47	−13.88
Δ^2E_{G3G4}	−10.68	−11.49	Δ^2E_{G3G4}	−12.84	−13.36	Δ^2E_{G3G4}	−13.46	−13.88
Δ^2E_{G2G3}	−10.68	−11.48	Δ^2E_{G2G3}	−12.84	−13.36	Δ^2E_{G2G3}	−13.45	−13.87
Δ^2E_{G2G4}	0.16	−0.37	Δ^2E_{G2G4}	−1.09	−1.34	Δ^2E_{G2G4}	−1.38	−1.53
Δ^5E	−37.71	−22.32	Δ^5E	−18.15	−2.84	Δ^5E	−5.47	−3.71
G-Be^{2+}			G-Ca^{2+}			G-Mg^{2+}		
Δ^2E_{iso}	−76.09	−74.91	Δ^2E_{iso}	−76.09	−74.91	Δ^2E_{iso}	−76.09	−74.91
ΔE_{Tot}	−588.85	−595.29	ΔE_{Tot}	−111.69	−119.99	ΔE_{Tot}	−456.09	−463.33
$\Delta^2E^{com}_{(G1+Be^{2+})}$	−251.05	−228.11	$\Delta^2E^{com}_{(G1^+Ca^{2+})}$	−109.95	−98.65	$\Delta^2E^{com}_{(G1^+Mg^{2+})}$	−155.29	−137.13
$\Delta^2E^{com}_{(G2^+Be^{2+})}$	−251.03	−228.10	$\Delta^2E^{com}_{(G2^+Ca^{2+})}$	−109.97	−98.66	$\Delta^2E^{com}_{(G2^+Mg^{2+})}$	−155.24	−137.17
$\Delta^2E^{com}_{(G3^+Be^{2+})}$	−251.02	−228.11	$\Delta^2E^{com}_{(G3^+Ca^{2+})}$	−109.98	−98.66	$\Delta^2E^{com}_{(G3^+Mg^{2+})}$	−155.39	−137.18
$\Delta^2E^{com}_{(G4^+Be^{2+})}$	−251.02	−228.13	$\Delta^2E^{com}_{(G4^+Ca^{2+})}$	−109.97	−98.66	$\Delta^2E^{com}_{(G4^+Mg^{2+})}$	−155.38	−137.12
Δ^2E_{G1G2}	−5.64	−7.46	Δ^2E_{G1G2}	−12.11	−13.08	Δ^2E_{G1G2}	−9.50	−10.84
Δ^2E_{G1G3}	6.81	5.02	Δ^2E_{G1G3}	−0.57	−0.91	Δ^2E_{G1G3}	0.56	−0.08
Δ^2E_{G1G4}	−5.61	−7.44	Δ^2E_{G1G4}	−12.10	−13.12	Δ^2E_{G1G4}	−9.51	−10.79
Δ^2E_{G3G4}	−5.63	−7.43	Δ^2E_{G3G4}	−12.10	−13.08	Δ^2E_{G3G4}	−9.47	−10.80
Δ^2E_{G2G3}	−5.66	−7.44	Δ^2E_{G2G3}	−12.09	−13.06	Δ^2E_{G2G3}	−9.55	−10.77
Δ^2E_{G2G4}	6.80	5.03	Δ^2E_{G2G4}	−0.57	−0.92	Δ^2E_{G2G4}	0.56	−0.086
Δ^5E	−424.2	−346.92	Δ^5E	−377.72	−328.81	Δ^5E	−204.36	−128.64

Table 2
Interaction energies ΔE (in kcal/mol) of alkali and alkaline earth metals with SG-tetrad complexes and their respective isolated SG-tetrad.

Base Pair	ΔE Kcal/mol		Base Pair	ΔE Kcal/mol		Base Pair	ΔE Kcal/mol	
	B3lyp	Mp2		B3lyp	Mp2		B3lyp	Mp2
6thioG-Li^+			6thioG-Na^+			6thio G-K^+		
Δ^2E_{iso}	−54.72	−59.67	Δ^2E_{iso}	−54.72	−59.67	Δ^2E_{iso}	−54.72	−59.67
ΔE_{Tot}	−170.35	−172.08	ΔE_{Tot}	−150.78	−149.01	ΔE_{Tot}	−128.83	−130.63
$\Delta^2E^{com}_{(G1^+Li^+)}$	−44.50	−42.09	$\Delta^2E^{com}_{(G1^+Na^+)}$	−34.77	−30.92	$\Delta^2E^{com}_{(G1^+K^+)}$	−24.22	−22.39
$\Delta^2E^{com}_{(G2^+Li^+)}$	−45.98	−43.15	$\Delta^2E^{com}_{(G2^+Na^+)}$	−34.78	−30.97	$\Delta^2E^{com}_{(G2^+K^+)}$	−24.20	−22.38
$\Delta^2E^{com}_{(G3^+Li^+)}$	−44.77	−41.84	$\Delta^2E^{com}_{(G3^+Na^+)}$	−34.83	−30.95	$\Delta^2E^{com}_{(G3^+K^+)}$	−24.23	−22.39
$\Delta^2E^{com}_{(G4^+Li^+)}$	−45.97	−43.15	$\Delta^2E^{com}_{(G4^+Na^+)}$	−34.79	−30.92	$\Delta^2E^{com}_{(G4^+K^+)}$	−24.20	−22.38
Δ^2E_{G1G2}	−9.45	−10.77	Δ^2E_{G1G2}	−10.44	−11.74	Δ^2E_{G1G2}	−10.55	−11.83
Δ^2E_{G1G3}	−0.22	−0.67	Δ^2E_{G1G3}	−0.51	−0.85	Δ^2E_{G1G3}	−0.65	−0.94
Δ^2E_{G1G4}	−9.83	−11.04	Δ^2E_{G1G4}	−10.42	−11.74	Δ^2E_{G1G4}	−10.56	−11.85
Δ^2E_{G3G4}	−9.49	−10.72	Δ^2E_{G3G4}	−10.45	−11.72	Δ^2E_{G3G4}	−10.55	−11.85
Δ^2E_{G2G3}	−9.84	−11.02	Δ^2E_{G2G3}	−10.44	−11.74	Δ^2E_{G2G3}	−10.56	−0.95
Δ^2E_{G2G4}	−0.13	−0.63	Δ^2E_{G2G4}	−0.51	−0.85	Δ^2E_{G2G4}	−0.66	−11.83
Δ^5E	−49.83	−43	Δ^5E	−31.16	−23.39	Δ^5E	−11.55	−8.16
6thio G-Be^{2+}			6thio G-Ca^{2+}			6thio G-Mg^{2+}		
Δ^2E_{iso}	−54.72	−59.67	Δ^2E_{iso}	−54.72	−59.67	Δ^2E_{iso}	−54.72	−59.67
ΔE_{Tot}	−549.45	−556.02	ΔE_{Tot}	−303.31	−314.52	ΔE_{Tot}	−403.68	−397.41
$\Delta^2E^{com}_{(G1^+Be^{2+})}$	−255.79	−242.09	$\Delta^2E^{com}_{(G1^+Ca^{2+})}$	−105.76	−94.97	$\Delta^2E^{com}_{(G1^+Mg^{2+})}$	−163.09	−147.53
$\Delta^2E^{com}_{(G2^+Be^{2+})}$	−255.72	−242.01	$\Delta^2E^{com}_{(G2^+Ca^{2+})}$	−105.73	−94.99	$\Delta^2E^{com}_{(G2^+Mg^{2+})}$	−163.05	−147.49
$\Delta^2E^{com}_{(G3^+Be^{2+})}$	−255.80	−242.10	$\Delta^2E^{com}_{(G3^+Ca^{2+})}$	−105.75	−95.00	$\Delta^2E^{com}_{(G3^+Mg^{2+})}$	−163.05	−147.49
$\Delta^2E^{com}_{(G4^+Be^{2+})}$	−255.78	−242.09	$\Delta^2E^{com}_{(G4^+Ca^{2+})}$	−105.76	−95.00	$\Delta^2E^{com}_{(G4^+Mg^{2+})}$	−163.06	−147.49
Δ^2E_{G1G2}	−9.32	−11.47	Δ^2E_{G1G2}	−10.70	−11.98	Δ^2E_{G1G2}	−9.61	−10.84
Δ^2E_{G1G3}	−5.35	4.19	Δ^2E_{G1G3}	−0.298	−0.66	Δ^2E_{G1G3}	0.14	−0.37
Δ^2E_{G1G4}	−9.33	−11.49	Δ^2E_{G1G4}	−10.69	−11.98	Δ^2E_{G1G4}	−9.60	−10.84
Δ^2E_{G3G4}	−9.32	−11.47	Δ^2E_{G3G4}	−10.68	−11.99	Δ^2E_{G3G4}	−9.58	−10.81
Δ^2E_{G2G3}	−9.30	−11.46	Δ^2E_{G2G3}	−10.69	−11.96	Δ^2E_{G2G3}	−9.60	−10.83
Δ^2E_{G2G4}	−5.32	4.16	Δ^2E_{G2G4}	−0.298	−0.66	Δ^2E_{G2G4}	0.14	−0.37
Δ^5E	−500.22	−449.81	Δ^5E	−163.05	−114.67	Δ^5E	−286.68	−236.65

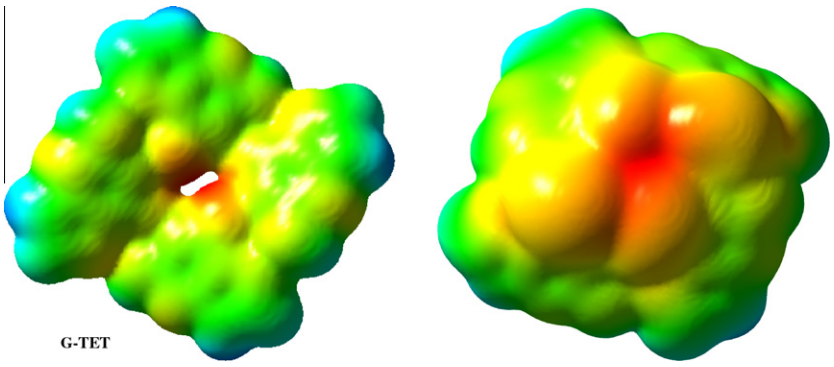

Fig. 4. Electrostatic potential of the G and SG-tetrads mapped onto the surface of the electron density of 0.002 unit calculated at B3LYP/6-311G** level of theory.

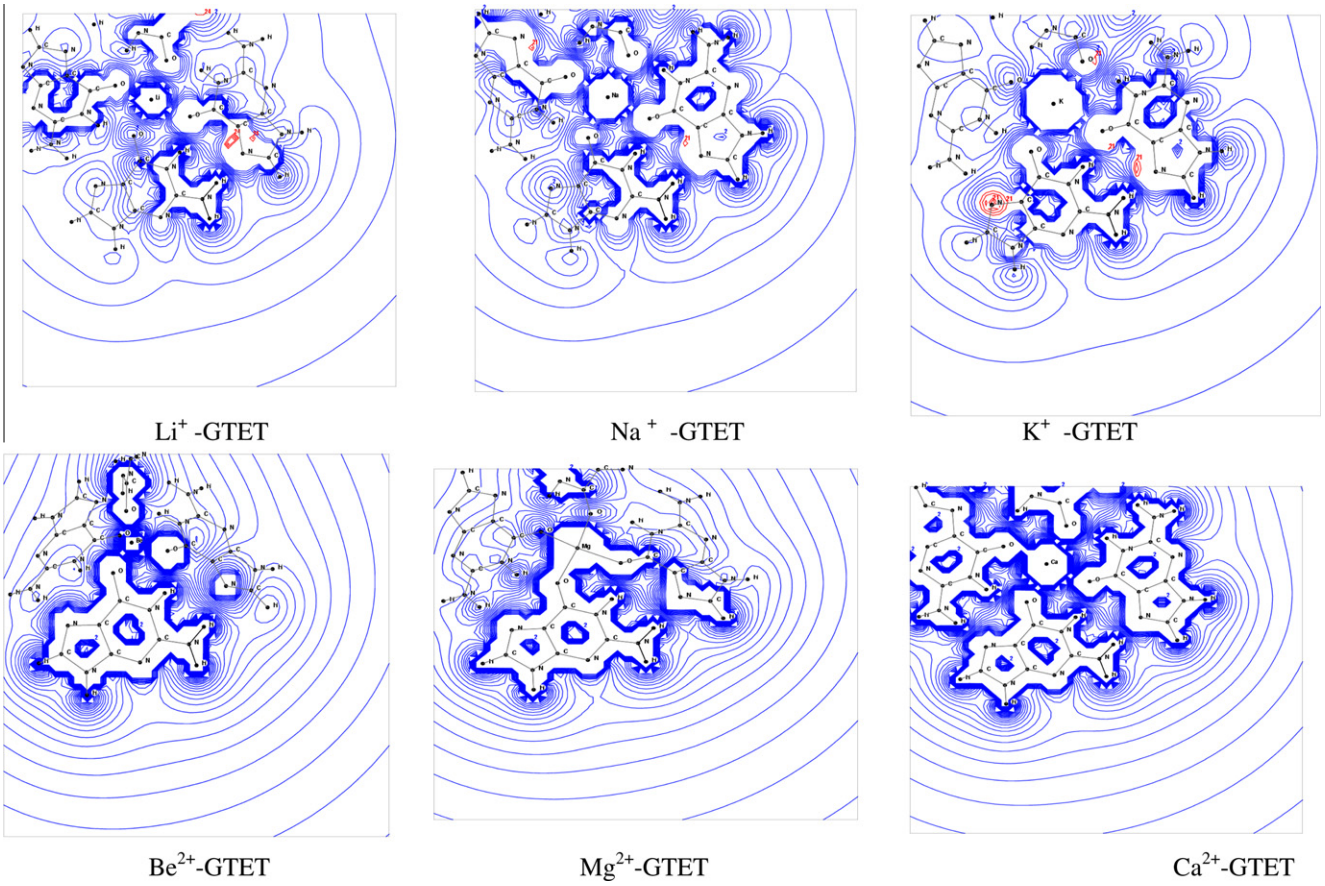

Fig. 5. Electrostatic potential of the G-tetrad mapped onto the surface of the electron density of 0.002 unit.

($\varepsilon = 78.5$) were calculated at B3LYP/6-311G** level of theory. The total energy reveals that the solvent interaction with the molecular system has increased the stability of the isolated tetrads and complexes. The stability order is found to be same as gas and aqueous phases. The dipole moment variations for alkali and alkaline earth metal complexes in both gas and aqueous phases have been depicted in Fig 3. It shows that irrespective of the medium, the dipole moment calculated for K^+, Be^{2+} and Mg^{2+} in G-tetrad, Na^+ and Mg^{2+} in SG-tetrad is found to have large dipole moment value. The structural distortion induced by the alkali and alkaline earth metals significantly changes the volume of the isolated G and SG-tetrads. The volume of the G-tetrads increases significantly from Li^+ to Na^+, Be^{2+} to Mg^{2+}, except K^+–G-tetrad Complexes. Whereas in case of SG-tetrad the volume of the tetrad decreases significantly from Li^+ to Na^+, and increases from Be^{2+} to Mg^{2+} complexes. The volume of G-tetrad are 352.38, 322.02, 390.19 and 339.47, 343.32, 364.09 (cm^3/mol) for Li^+, Na^+, K^+ and Be^{2+}, Ca^{2+}, Mg^{2+} interacting complexes respectively. Similarly for SG-tetrad the volumes are 449.43, 395.24, 427.32 and 369.59, 398.15, 496.21 (cm^3/mol) for Li^+, Na^+, K^+ and Be^{2+}, Ca^{2+}, Mg^{2+} interacting complexes respectively at B3LYP/6-311G** level of theory.

3.2. Interaction energy and metal ion affinity

The calculated interaction energies of the studied systems are summarized in Tables 1 and 2. The interaction energies of G-tetrad is −76.09 and −74.91 kcal/mol, more stable than that of SG-tetrad of −54.72 and −59.67 kcal/mol at B3LYP/6-311G** and MP2/6-

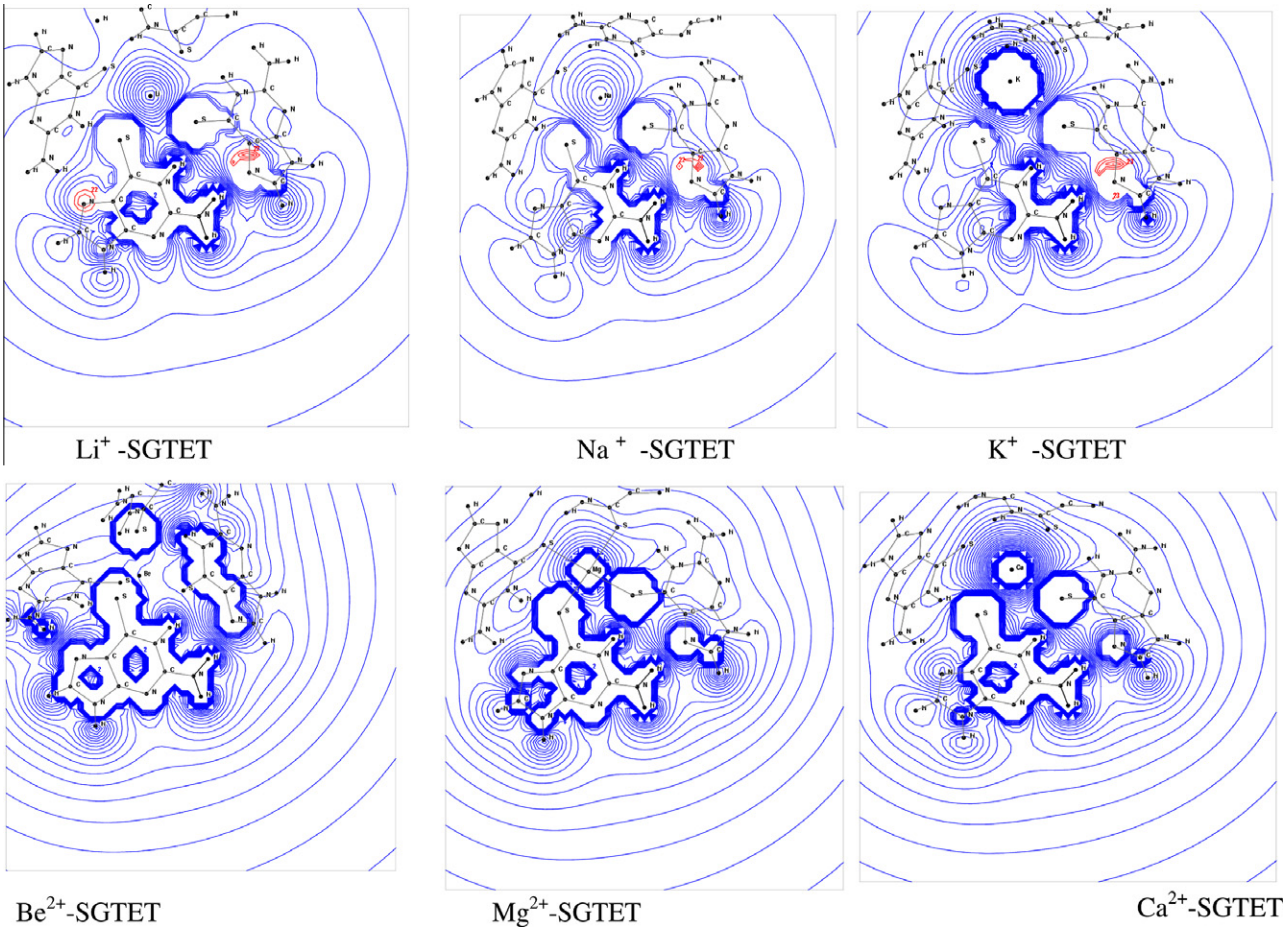

Fig. 6. Electrostatic potential of the SG-tetrad mapped onto the surface of the electron density of 0.002 unit.

311G** levels of theory respectively. The SG-tetrad is less stable than G-tetrad due to the sulfur atom and the interaction energy decreases around −21.37 and −15.24 kcal/mol at the above level of theory. Olivas and Maher [48] and others [49,50] indicate that 6-thioguanine alters the structure and stability of duplex DNA and inhibits quadruplex DNA formation, due to the increased radius and the decreased electronegativity of the sulfur, which would destabilize the Hoogsteen hydrogen bonding of guanine quartets relative to Watson–Crick pairing. In the case of G and SG-tetrads, the Li^+ cation, which has the smallest size, has the biggest interaction energy of −205.48, −209.69 and −170.35, −172.08 kcal/mol at B3LYP/6-311G** and MP2/6-311G** levels of theory respectively. It could be seen that the interaction of the Na^+–G-tetrad is much stronger than that of the K^+–G-tetrad. It is clear that these kinds of trends are consistent with the changes in the hydrogen bonding, as discussed above. In case of alkaline earth metal cation Be^{2+}–G and SG-tetrads are found to have strong interaction energy of −588.85, −595.29 and −549.45, −556.02 kcal/mol at the above levels of theory respectively. Similar results are predicted by the metal ion affinity and follow the same trend. The metal ion affinity values of G-tetrad are −128.58, −107.07, −80.32 for Li^+, Na^+, K^+ complexes and −494.99, −370.99, −281.36 for Be^{2+}, Mg^{2+}, Ca^{2+} complexes respectively. In case of SG-tetrad the metal ion affinity values are −109.83, −90.65, −68.44 for Li^+, Na^+, K^+ and −476.48, −348.72, −260.27 for Be^{2+}, Mg^{2+}, Ca^{2+} complexes respectively.

The interaction energy and metal ion affinity stability order is $Li^+ > Na^+ > K^+$, $Be^{2+} > Mg^2 > Ca^{2+}$ interacting complexes. It is found that the smaller the size of metal ion, the larger the respective interaction energy and metal ion affinity. From the structural properties it is clear that complex having higher interaction energy is more distorted than the other complexes. For all the metal interacting complexes the two body interaction energies are found to be higher compared with any other two body interactions, which is the reason for higher stability of the complexes. It is observed that the $\Delta^2 E_{G1G3}$ for Li^+, Be^{2+} and Mg^{2+} in G and SG-tetrads is found to be positive indicating the absence of interaction. Notably, it is observed that the many body interaction energy ($\Delta^3 E$) is negative for all the metal complexes except Li^+ and Mg^{2+} complexes, which shows the strongest many body interaction in these complexes.

3.3. Electrostatic potential map

The electrostatic potentials (ESPs) reveal important information on properties of the studied systems. Electrostatic properties of nucleotides govern the orientational dependence of stacking interactions and may also be important for the fidelity of DNA polymerase. Chin et al. [51] proposed that the electrostatic potential might play an important role in nucleic acid recognition and stabilization. Sites of unusual electrostatic features correspond to functionally important regions, for example, binding sites for metal ions characterized by a usually negative electrostatic potential. The electrostatic potential maps has been plotted for G, SG-tetrads and their alkali, alkaline earth metal interacting complexes and are shown in Figs. 4–6.

The electrostatic potential map of G-tetrad shows significant concentration of the negative charge in the central area of G-tetrad (Fig. 4). The effect of cation in stabilizing G-tetrad is clearly through the neutralization of this charge [52]. The projection of the electrostatic potential on the 0.002 electron density surface

Table 3
Electron density ρ (in a.u.), Laplacian of electron density $\nabla^2\rho$ (in a.u) and Ellipticity corresponds to interactions in metal interacting complexes at B3LYP/6-311G** level of theory

	ρ	$\nabla^2\rho$	ε		ρ	$\nabla^2\rho$	ε		ρ	$\nabla^2\rho$	ε
Li^+–Gtetrad				**Na^+–Gtetrad**				**K^+–Gtetrad**			
N_{50}–H_{49}...N_{28}	0.030	0.088	0.060	N_{50}–H_{49}...N_{28}	0.030	0.088	0.056	N_{50}–H_{49}...N_{28}	0.030	0.089	0.057
N_{53}–H_{54}...O_{24}	0.035	0.119	0.039	N_{53}–H_{54}...O_{24}	0.030	0.105	0.328	N_{53}–H_{54}...O_{24}	0.026	0.096	0.031
N_{18}–H_{19}...N_{12}	0.031	0.088	0.060	N_{18}–H_{19}...N_{12}	0.031	0.088	0.055	N_{18}–H_{19}...N_{12}	0.030	0.088	0.057
N_{21}–H_{22}...O_8	0.036	0.119	0.039	N_{21}–H_{22}...O_8	0.030	0.105	0.028	N_{21}–H_{22}...O_8	0.027	0.095	0.032
N_2–H_3...N_{44}	0.030	0.088	0.060	N_2–H_3...N_{44}	0.031	0.088	0.056	N_2–H_3...N_{44}	0.031	0.089	0.057
N_5–H_6...O_{40}	0.035	0.119	0.039	N_5–H_6...O_{40}	0.030	0.105	0.028	N_5–H_6...O_{40}	0.027	0.094	0.030
N_{34}–H_{33}...N_{60}	0.030	0.088	0.060	N_{34}–H_{33}...N_{60}	0.031	0.088	0.056	N_{34}–H_{33}...N_{60}	0.031	0.089	0.057
N_{37}–H_{38}...O_{56}	0.035	0.119	0.039	N_{37}–H_{38}...O_{56}	0.030	0.105	0.028	N_{37}–H_{38}...O_{56}	0.026	0.095	0.033
C_{55}–O_{56}...Li_{65}	0.020	0.139	0.057	C_{55}–O_{56}...Na_{65}	0.022	0.139	0.029	C_{55}–O_{56}...K_{65}	0.021	0.098	0.043
C_{23}–O_{24}...Li_{65}	0.020	0.140	0.056	C_{23}–O_{24}...Na_{65}	0.022	0.139	0.029	C_{23}–O_{24}...K_{65}	0.021	0.099	0.041
C_7–O_8...Li_{65}	0.020	0.139	0.057	C_7–O_8...Na_{65}	0.022	0.139	0.029	C_7–O_8...K_{65}	0.021	0.098	0.044
C_{39}–O_{40}...Li_{65}	0.020	0.139	0.056	C_{39}–O_{40}...Na_{65}	0.022	0.139	0.029	C_{39}–O_{40}...K_{65}	0.021	0.098	0.039
Li^+–SGtetrad				**Na^+–SGtetrad**				**K^+–SGtetrad**			
N_{50}–H_{49}...N_{28}	0.023	0.071	0.062	N_{50}–H_{49}...N_{28}	0.022	0.068	0.063	N_{50}–H_{49}...N_{28}	0.021	0.067	0.063
N_{53}–H_{54}...S_{24}	0.027	0.054	0.057	N_{53}–H_{54}...S_{24}	0.022	0.048	0.061	N_{53}–H_{54}...S_{24}	0.019	0.045	0.058
N_{18}–H_{19}...N_{12}	0.027	0.067	0.061	N_{18}–H_{19}...N_{12}	0.022	0.068	0.063	N_{18}–H_{19}...N_{12}	0.021	0.068	0.063
N_{21}–H_{22}...S_8	0.027	0.056	0.066	N_{21}–H_{22}...S_8	0.022	0.048	0.061	N_{21}–H_{22}...S_8	0.019	0.045	0.057
N_2–H_3...N_{44}	0.023	0.071	0.062	N_2–H_3...N_{44}	0.022	0.068	0.063	N_2–H_3...N_{44}	0.021	0.067	0.063
N_5–H_6...S_{40}	0.027	0.054	0.057	N_5–H_6...S_{40}	0.022	0.048	0.061	N_5–H_6...S_{40}	0.019	0.045	0.058
N_{34}–H_{33}...N_{60}	0.022	0.067	0.060	N_{34}–H_{33}...N_{60}	0.021	0.068	0.062	N_{34}–H_{33}...N_{60}	0.021	0.068	0.063
N_{37}–H_{38}...S_{56}	0.027	0.056	0.065	N_{37}–H_{38}...S_{56}	0.021	0.048	0.061	N_{37}–H_{38}...S_{56}	0.019	0.045	0.057
C_{55}–S_{56}...Li_{65}	0.015	0.068	0.139	C_{55}–S_{56}...Na_{65}	0.015	0.066	0.066	C_{55}–S_{56}...K_{65}	0.013	0.047	0.074
C_{23}–S_{24}...Li_{65}	0.013	0.059	0.200	C_{23}–S_{24}...Na_{65}	0.015	0.066	0.066	C_{23}–S_{24}...K_{65}	0.013	0.047	0.074
C_7–S_8...Li_{65}	0.015	0.068	0.141	C_7–S_8...Na_{65}	0.015	0.065	0.066	C_7–S_8...K_{65}	0.013	0.047	0.074
C_{39}–S_{40}...Li_{65}	0.013	0.058	0.211	C_{39}–S_{40}...Na_{65}	0.015	0.065	0.065	C_{39}–S_{40}...K_{65}	0.013	0.047	0.074
Be^{2+}–Gtetrad				**Mg^{2+}–Gtetrad**				**Ca^{2+}–Gtetrad**			
N_{50}–H_{49}...N_{28}	0.019	0.059	0.069	N_{50}–H_{49}...N_{28}	0.028	0.084	0.061	N_{50}–H_{49}...N_{28}	0.029	0.086	0.059
N_{53}–H_{54}...O_{24}	0.030	0.111	0.062	N_{53}–H_{54}...O_{24}	0.028	0.098	0.047	N_{53}–H_{54}...O_{24}	0.021	0.073	0.033
N_{18}–H_{19}...N_{12}	0.019	0.059	0.069	N_{18}–H_{19}...N_{12}	0.028	0.084	0.061	N_{18}–H_{19}...N_{12}	0.029	0.086	0.059
N_{21}–H_{22}...O_8	0.030	0.110	0.062	N_{21}–H_{22}...O_8	0.028	0.098	0.047	N_{21}–H_{22}...O_8	0.021	0.073	0.033
N_2–H_3...N_{44}	0.019	0.059	0.069	N_2–H_3...N_{44}	0.028	0.083	0.060	N_2–H_3...N_{44}	0.029	0.086	0.059
N_5–H_6...O_{40}	0.030	0.109	0.062	N_5–H_6...O_{40}	0.028	0.098	0.046	N_5–H_6...O_{40}	0.021	0.079	0.033
N_{34}–H_{33}...N_{60}	0.019	0.059	0.069	N_{34}–H_{33}...N_{60}	0.028	0.084	0.061	N_{34}–H_{33}...N_{60}	0.029	0.086	0.059
N_{37}–H_{38}...O_{56}	0.030	0.110	0.062	N_{37}–H_{38}...O_{56}	0.028	0.099	0.047	N_{37}–H_{38}...O_{56}	0.021	0.073	0.033
C_{55}–O_{56}...Be_{65}	0.066	0.465	0.094	C_{55}–O_{56}...Mg_{65}	00.41	0.326	0.029	C_{55}–O_{56}...Ca_{65}	0.045	0.253	0.065
C_{23}–O_{24}...Be_{65}	0.066	0.465	0.094	C_{23}–O_{24}...Mg_{65}	0.041	0.327	0.029	C_{23}–O_{24}...Ca_{65}	0.045	0.253	0.065
C_7–O_8...Be_{65}	0.066	0.465	0.094	C_7–O_8...Mg_{65}	0.041	0.326	0.029	C_7–O_8...Ca_{65}	0.045	0.253	0.065
C_{39}–O_{40}...Be_{65}	0.066	0.465	0.094	C_{39}–O_{40}...Mg_{65}	0.041	0.327	0.029	C_{39}–O_{40}...Ca_{65}	0.045	0.253	0.065
Be^{2+}–SGtetrad				**Mg^{2+}–SGtetrad**				**Ca^{2+}–SGtetrad**			
N_{50}–H_{49}...N_{28}	0.019	0.062	0.056	N_{50}–H_{49}...N_{28}	0.021	0.065	0.065	N_{50}–H_{49}...N_{28}	0.019	0.063	0.064
N_{53}–H_{54}...S_{24}	0.026	0.055	0.023	N_{53}–H_{54}...S_{24}	0.028	0.057	0.073	N_{53}–H_{54}...S_{24}	0.022	0.049	0.066
N_{18}–H_{19}...N_{12}	0.019	0.062	0.056	N_{18}–H_{19}...N_{12}	0.021	0.065	0.066	N_{18}–H_{19}...N_{12}	0.019	0.062	0.064
N_{21}–H_{22}...S_8	0.026	0.055	0.023	N_{21}–H_{22}...S_8	0.028	0.057	0.073	N_{21}–H_{22}...S_8	0.022	0.049	0.066
N_2–H_3...N_{44}	0.019	0.062	0.056	N_2–H_3...N_{44}	0.021	0.064	0.065	N_2–H_3...N_{44}	0.019	0.063	0.064
N_5–H_6...S_{40}	0.026	0.055	0.022	N_5–H_6...S_{40}	0.028	0.057	0.073	N_5–H_6...S_{40}	0.022	0.049	0.066
N_{34}–H_{33}...N_{60}	0.019	0.061	0.056	N_{34}–H_{33}...N_{60}	0.021	0.068	0.065	N_{34}–H_{33}...N_{60}	0.020	0.063	0.064
N_{37}–H_{38}...S_{56}	0.026	0.055	0.023	N_{37}–H_{38}...S_{56}	0.028	0.057	0.073	N_{37}–H_{38}...S_{56}	0.022	0.049	0.066
C_{55}–S_{56}...Be_{65}	0.049	0.135	0.055	C_{55}–S_{56}...Mg_{65}	0.029	0.113	0.070	C_{55}–S_{56}...Ca_{65}	0.032	0.093	0.120
C_{23}–S_{24}...Be_{65}	0.049	0.135	0.054	C_{23}–S_{24}...Mg_{65}	–	–	–	C_{23}–S_{24}...Ca_{65}	0.032	0.093	0.120
C_7–S_8...Be_{65}	0.049	0.135	0.054	C_7–S_8...Mg_{65}	0.029	0.113	0.070	C_7–S_8...Ca_{65}	0.032	0.093	0.120
C_{39}–S_{40}...Be_{65}	0.049	0.135	0.054	C_{39}–S_{40}...Mg_{65}	–	–	–	C_{39}–S_{40}...Ca_{65}	0.032	0.093	0.120

clearly shows that the central area is the only location to host a cation for the G-tetrad. In the SG-tetrad the regions with the most negative electrostatic potential exist in the central cavity of the four sulfur atoms, where the cavity is much smaller than that of G-tetrad (Fig 4). As compared with carbonyl oxygen, sulfur atom has increased radius and decreased electronegativity, which causes the electron of sulfur diffuse more widely than carbonyl oxygen, thus the central cavity of SG-tetrad is smaller than that of G-tetrad. Also, hydrogen bonds involving SG shows a slightly reduced electrostatic contribution whereas the dispersion attraction is enhanced [7]. It could be seen that both the shape and the size of the negative cavity affect the binding of the cation.

For the alkali metal complexes, the delocalized charges are localized at the Li^+ ion and the charge decreasing trend has been observed for Na^+ and K^+ complexes as shown in Figs 5 and 6. Similarly, the charge decreasing trend has been observed for the alkaline earth metal complexes (Be^{2+}, Mg^{2+} and Ca^{2+}). The overlapping of the charges between electronegative atoms and metal ions in the G and SG-tetrads decreases as moving from Li^+ to K^+ and also from Be^{2+} to Ca^{2+} complexes. Hence, the electron density of the G-tetrad with metal ion is found to be decreased for K^+ and Ca^{2+} complexes. It is worth to note that while moving from Li^+ to K^+ and also from Be^{2+} to Ca^{2+} metal complexes, the positive nature of the metal ion charges in the complexes are also found to be increased as the coordination distance increased (overlapping of charges are decreased). This result confirms that the amount of charges transferred from the G and SG-tetrads to metal ions decreases as moving from Li^+ to Ca^{2+} metal complexes, which

agree well with the previous charge analyses studied by our group [45].

3.4. Topological analysis

The interactions are studied by considering the values of the electron density (ρ), its Laplacian ($\nabla^2\rho$) and bond ellipticity (ε) at the bond critical points (BCP) in the complexes and are summarized in Table 3. It is expected that the strong bonds are usually associated with higher electron density, indicating higher structural stability, as is observed for N–H···N, N–H···O and N–H···S interactions in tetrads. The (ρ) and ($\nabla^2\rho$) calculated for C–O/S···M (M = Li^+, Na^+, K^+, Be^{2+}, Mg^{2+} and Ca^{2+}) interactions are found to be very small, while comparing the above values with N–H···N, N–H···O and N–H···S type hydrogen bonds. The (ρ) and ($\nabla^2\rho$) at N–H···O is larger than N–H···N for all the complexes with S_4 symmetry. This is because an S_4 structure make the M···O distance possible to come closer, thus making the N–H···O distance smaller and N–H···N distance longer, and further cause the N–H···O strengthen and N–H···N weakens. As expected, the (ρ) and ($\nabla^2\rho$) are decreases as the hydrogen bond length increases. The electron densities of N–H···O interactions are found to be higher than that of N–H···S interactions. As discussed previously sulfur atom has increased radius and decreased electronegativity compared with carbonyl oxygen, which causes the electron of sulfur diffuse more widely than carbonyl oxygen. For alkali and alkaline earth metal complexes, as the ionic radius of the metal cation increases from Li^+ to K^+ and from Be^{2+} to Ca^{2+} complexes the interactions between M···O6 and M···S6 increases, hence the (ρ) and ($\nabla^2\rho$) values are found to decrease. The electron density values calculated at the BCPs augment the stability order predicted through the interaction energy and the coordination distance.

4. Conclusions

The optimized structures of the G, SG-tetrads and their alkali, alkaline earth metal ion interacting complexes were studied by ab initio and density functional theory methods. The SG-tetrad has less compact structure than G-tetrad due to the presence of larger radius sulfur atom in SG-tetrad. The smaller ions are more tightly bonded to G and SG-tetrads suggesting the domination of the electrostatic interaction in the cation–tetraplexes systems The SG-tetrad is less stable than G-tetrad due to the sulfur atoms and the interaction energy decreases around −21.37 and −15.24 kcal/mol as moving from G to SG-tetrads at B3LYP and MP2 methods. The interaction energy and metal ion affinity stability order is Li^+>Na^+>K^+, Be^{2+}>Mg^2>Ca^{2+} interacting complexes. It is found that the smaller the size of metal ion, the larger the respective interaction energy and metal ion affinity. But as moving from Li^+ to Be^{2+} complexes the interaction energy and metal ion affinity increases. The electrostatic potential map reveals that the amount of charges transferred from the G and SG-tetrads to metal ion decreases as moving from Li^+ to Ca^{2+} metal complexes. From the Topological analysis, it is observed that for alkali and alkaline earth metal complexes, as the ionic radius of the metal cation increases from Li^+ to K^+ and from Be^{2+} to Ca^{2+} complexes the interactions between M···O6 and M···S6 increases, hence the (ρ) and ($\nabla^2\rho$) values are found to decrease.

Acknowledgment

One of the authors P. Deepa expresses her sincere thanks to CSIR, New Delhi, for the award of Senior Research Fellowship.

Appendix A. Supplementary data

Supplementary data associated with this article can be found, in the online version, at doi:10.1016/j.comptc.2011.07.012.

References

[1] W. Guschlbauer, J.F. Chantot, D. Thiele, J. Biomol. Struct. Dyn. 3 (1990) 491.
[2] J. Suhnel, Biopolymers 61 (2002) 32.
[3] M. Meyer, J. Sühnel, in: J. Leszczynski (Ed.), Computational Chemistry: Reviews of Current Trends, vol. 8, World Scientific, 2003, pp. 161–208. ISBN 981-238-702-1 (chapter 4).
[4] D.J. Patel, S. Bouaziz, A. Kettanim, Y. Wang, Structures of guanine-rich and cytosine-rich quadruplexes formed in vito by telomeric, centromeric and triplet repeat disease DNA sequences, in: D. Neidle (Ed.), The Oxford Handbook of Nucleic Acid Structure, OUP, Oxford, 1999, pp. 389–453.
[5] E. Mezzina, P. Mariani, R. Itri, S. Masiero, S. Pieraaccini, G.P. Spada, F. Spinozzi, J.T. Davis, G. Gottarelli, Chem. Eur. J. 7 (2002) 388.
[6] A.M. Zahler, J.R. Williamson, T.R. Cech, D.M. Prescott, Nature 350 (1991) 718.
[7] F. Meng, W. Xu, C. Li, Chem. Phys. Lett. 389 (2004) 421.
[8] R. Stefl, N. Spackova, I. Berger, J. Koca, J. Sponer, Biophys. J. 80 (2001) 455.
[9] V.M. Marathias, M.J. Sawicki, P.H. Bolton, Nucl. Acid Res. 27 (1999) 2860.
[10] W.S. Ross, C.C. Hardin, J. Am. Chem. Soc. 116 (1994) 6070.
[11] J. Tohl, W. Eimer, Biophys. Chem. 67 (1997) 177.
[12] J.M. Darlow, D.R.F. Leach, J. Mol. Biol. 275 (1998) 3.
[13] C. Harrington, Y. Lan, S.A. Akman, J. Biol. Chem. 272 (1997) 24631.
[14] G. Laughlan, A.I. H. Murchie, D.G. Norman, M.H. Moore, P.C.E. Moody, D.M.J. Lilley, B. Luisi, Science 265 (1994) 520.
[15] K. Philips, Z. Dauter, A.I.H. Murchie, D.M.J. Lilley, B. Luisi, J. Mol. Biol. 273 (1997) 171.
[16] N. Nagesh, D. Chatterji, J. Biochem. Biophys. Methods 30 (1995) 1.
[17] J.R. Williamson, Annu. Rev. Biophys. Biomol. Struct. 23 (1994) 703.
[18] W.I. Sundquist, A. Klung, Nature 342 (1989) 825.
[19] N. Spackova, I. Berger, J. Sponer, J. Am. Chem. Soc. 121 (1999) 5519.
[20] N. Jing, W. Xiong, Y. Guan, L. Pallansch, S. Wang, Biochemistry 41 (2002) 5397.
[21] J. Gu, J. Leszczynski, M. Bansal, Chem. Phys. Lett. 311 (1999) 209.
[22] J. Gu, J. Leszczynski, J. Phys. Chem. A 104 (2000) 6308.
[23] J. Leszczynski, J. Phys. Chem. A 102 (1998) 2357.
[24] L. Gorb, J. Leszczynski, J. Am. Chem. Soc. 120 (1998) 504.
[25] N.U. Zhanpeisov, J. Sponer, J. Leszczynski, J. Phys. Chem. A 102 (1998) 10374.
[26] M. Meyer, C. Schneider, M. Brandl, J. Suhnel, J. Phys. Chem. A 105 (2001) 11560.
[27] I. Bertini, C. Luchinat, in: M.H.E. Clementi, G. Corongiu, M.H. Sarma, R.H. Sarma (Eds.), Structures & Motion: Membranes, Nucleic Acids & Proteins, Adenine Press, Guilderland, NY, 1985, pp. 293–329.
[28] P. Deepa, P. Kolandaivel, J. Biomol. Struct. Dyn. 25 (2008) 1.
[29] P. Deepa, P. Kolandaivel, K. Senthilkumar, Biophys. Chem. 136 (2008) 50.
[30] P. Deepa, P. Kolandaivel, K. Senthilkumar, Int. J. Quant. Chem. 111 (2011) 3239.
[31] P. Deepa, P. Kolandaivel, K. Senthilkumar, Polyhderon 30 (2011) 1431.
[32] C. Moller, M.S. Plesset, Phys. Rev. 46 (1934) 618.
[33] A.D. Becke, Phys. Rev. A 38 (1988) 3098.
[34] C. Lee, W. Yang, R.G. Parr, Phys. Rev. B 37 (1988) 785.
[35] S. Miertus, E. Scrocco, J. Tomasi, J. Chem. Phys. 55 (1981) 117.
[36] S.F. Boys, F. Bernardi, Mol. Phys. 19 (1970) 553.
[37] S.S. Xantheas, J. Chem. Phys. 104 (1996) 8821.
[38] R.F.W. Bader, Atoms in Molecules, A Quantum Theory, Clarendon Press, London, 1990.
[39] P.L.A. Popelier, R.F.W. Bader, Chem. Phys. Lett. 189 (1992) 542.
[40] J.R. Cheeseman, M.T. Caroll, R.F.W. Bader, Chem. Phys. Lett. 143 (1988) 450.
[41] U. Koch, P.L.A. Popelier, J. Phys. Chem. 99 (1995) 9747.
[42] F. Meng, F. Wang, X. Zhao, A.F. Jalbout, J. Mol. Struct 854 (2008) 26.
[43] G. Louit, A. Hocquet, M. Ghomi, M. Meyer, J. Suhnel, Phys. Chem. Comm. 5 (2002) 94.
[44] P.C. Hariharan, J.A. Pople, Theor. Chim. Acta 28 (1973) 213.
[45] R. Shankar, P. Kolandaivel, L. Senthilkumar, J. Phy. Org. Chem (2010), doi:10.1002/POC.1786.
[46] M.J. Frisch, G.W. Trucks, H.B. Schlegel, G.E. Scuseria, M.A. Robb, J.R. Cheeseman, V.G. Zakrzewski, J.A. Montgomery Jr., R.E. Stratmann, J.C. Burant, S. Dapprich, J.M. Millam, A.D. Daniels, K.N. Kudin, M.C. Strain, O. Farkas, J. Tomasi, V. Barone, M. Cossi, R. Cammi, B. Mennucci, C. Pomelli, C. Adamo, S. Clifford, J. Ochterski, G.A. Petersson, P.Y. Ayala, Q. Cui, K. Morokuma, D.K. Malick, A.D. Rabuck, K. Raghavachari, J.B. Foresman, J. Cioslowski, J.V. Ortiz, A.G. Baboul, B.B. Stefanov, G. Liu, A. Liashenko, P. Piskorz, I. Komaromi, R. Gomperts, R.L. Martin, D.J. Fox, T. Keith, M.A. Al-Laham, C.Y. Peng, A. Nanayakkara, C. Gonzales, M. Challacombe, P.M.W. Gill, B. Johnson, W. Chen, M.W. Wong, J.L. Andres, C. Gonzalez, M. Head-Gordon, E.S. Replogle, J.A. Pople, Gaussian 03. Revision A.11. 2, Gaussian, Inc., Pittsburgh PA, 2005.
[47] W.S. Ross, C.C. Hardin, J. Am. Chem. Soc. 116 (1994) 6070.
[48] W.M. Olivas, L.J. Maher, Nucl. Acid Res. 23 (1995) 1936.
[49] T.S. Rao, T.H. Durland, D.M. Seth, M.A. Myrick, V. Bodepudi, G.R. Revankar, Biochemistry 34 (1995) 765.
[50] N.V. Hud, P. Schultze, J. Feigon, J. Am. Chem. Soc. 120 (1998) 6403.
[51] K. Chin, K.A. Sharp, B. Hoing, Nat. Struct. Biol. 6 (1999) 10551061.
[52] J.D. Gu, J. Leszczynski, M. Bansal, Chem. Phys. Lett. 311 (1999) 209.